



Synthesis and Characterization of β -Wollastonite from Limestone and Rice Husk as Reinforcement Filler for Clay Based Ceramic Tiles

Chirotaw Getem¹ and Nigus Gabbiye²(✉)

¹ School of Mechanical and Chemical Engineering, Kombolcha Institute of Technology,
Wollo University, P.O. Box 208, Kombolcha, Ethiopia
chiotawgetem@gmail.com

² Faculty of Chemical and Food Engineering, Bahir Dar Institute of Technology,
Bahir Dar University, P.O. Box 26, Bahir Dar, Ethiopia
nigushabtu@gmail.com

Abstract. This work focuses on the synthesis of β -Wollastonite and utilized as reinforcement filler for ceramic tile. β -Wollastonite was synthesized by taking the raw limestone as a lime precursor and rice husk as a source of silica. The lime and silica powders were mixed with 1:1 w/w ratio and then calcined at 900 °C for 4 h. The ceramic tiles were prepared by solid slip casting method for a wide range of β -wollastonite to clay ratio (5, 15 and 25%), particle size of 63, 75 and 125 μm at firing temperature of 950, 1000 and 1050 °C. The results show that a minimum linear shrinkage of 1.25% was recorded at 25% β -wollastonite-clay ratio with a particle size of 125 μm at a temperature of 950 °C. The ceramic tiles fabricated were exhibited minimum water absorption of 1.35% and maximum compressive strength of 38.35 MPa at 25% of β -wollastonite to clay ratio, particle size of 63 μm and 1050 °C firing temperature. Similarly, the maximum acid resistance of 99.985% was found on 75 and 125 μm particle sizes with a 25% ratio of β -Wollastonite and 950 °C firing temperature.

Keywords: Ceramic tile · Clay · β -wollastonite · Limestone · Rice husk

1 Introduction

Ceramic tiles are a thin slab, having a full cross-section, made from clays and/or other inorganic raw materials and an important construction material used in almost all construction sectors. The production of ceramic tiles starts from raw material, grinding and mixing and usually shaped at room temperature, then dried and subsequently fired at a temperature sufficient to develop the required properties [1]. The quality and cost of the final product of ceramic tiles depend on the composition of raw materials, firing cycle [2], mixing proportions [3] and particle size of the starting materials [4].

In developing countries, there is a great shortage of ceramic tile materials. For example, local materials are often used, like soil, stone, grass and palm leaves for roofs.

These roofs are characterized by their weak strength and have a low resistant to harsh environmental conditions such as rain. Currently, materials like corrugated iron sheets and asbestos cement sheets have replaced the traditional construction materials. The corrugated iron sheet roofs in tropical areas give a poor indoor climate and make a lot of noise when it rains and needs a lot of energy during their production. Asbestos cement sheets should not even be thought-about, due to health hazards [5].

Ceramic tiles are characterized by their weak plastic deformation properties, as a result, catastrophic failure takes place and also minor crack propagate quickly to critical sizes. Besides, ceramic tiles surfaces can allow water and contaminants to enter into and exit which often permeating into cavities behind the tiles, corroding the bonding agent, the substrate itself or perhaps the ceramic tile. It is very difficult to clean, over time they become dirty and have to be removed physically or mechanically; laborious and costly undertaking [6].

During the production of ceramic tile high amount of feldspars is added [7]. However, feldspar particles tend to stick to each other like socks with static cling from the dryer. Tiny bits of feldspar adhere to one another and resist being mixed into the clay body as individual particles. Therefore, replacing the existing material formulation of tiles and their properties by incorporating natural fibrous into its starting materials is a key step. Thus, in this research work the potential application of β -wollastonite as reinforcement filler for clay-based ceramic tile was investigated. β -wollastonite is composed of CaO and SiO₂ with the chemical formula of β -CaSiO₃ [8].

2 Materials and Methods

2.1 Materials and Chemicals

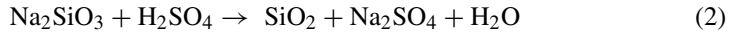
The primary raw materials were rice husk, limestone and clay. Rice husk was collected from local rice producers and millers located at Fogera Woreda, South Gonder, Ethiopia, where there is a high production of rice. Limestone and clay were collected from Abbay Gorge and Addis Zemen, Ethiopia, respectively. HCl (35.4%) was used for soaking of rice husk to remove soluble minerals. NaOH (97%) and H₂SO₄ (98%) were used for extraction of silica from rice husk ash and to extract silica gel from sodium silicate solution.

2.2 Methods

Extraction of Silica from Rice Husk (RH): Silica was extracted from RH by using alkaline extraction followed by acid precipitation [9]. RH was sieved and washed with water to removes dirties or impurities. Then, it was soaked in a solution of 1N HCl for 8 h to remove impurities attached on it and to make easy for calcination. After leached with HCl, it was washed again with distilled water until the pH became neutral. Then dried by sun light for about 48 h and calcined in an electric furnace at 700 °C for 6 h. 10 g of Rice Husk Ash (RHA) was dispersed in 60 ml, 2.5 M solution of NaOH for 2 h at 60 °C [10]. The silica content of the RHA leached out to the aqueous phase of the dispersion in the form of soluble sodium silicate according to Eq. 1 [11].



The resulting sodium silicate solution was filtered using 110 mm filter paper in a vacuumed filtration condition. The filtrate was allowed to cool to room temperature and then acidified with 2N H_2SO_4 , which precipitated the dissolved silicate in the form of white gelatinous solid with constant stirring to neutral pH. The precipitation using H_2SO_4 occurred according to Eq. 2 [12].



Silica gels started to precipitate when the pH decreased to less than 10 followed by aging for 20 h. The gels were then dried at 80 °C for 12 h.

Experimental Procedure for Preparation of Lime (CaO): Limestone was soaked for three days in distilled water. Then, it was removed and washed again to avoid unwanted impurities that attached on the surface and dried at 105 °C in an oven for 24 h. The dried limestone was subjected to a disk mill for size reduction (0.1 mm). Then, it was washed using distilled water to remove the remain and water-soluble components and dried at 105 °C for 24 h. and calcined at 950 °C in an electric furnace for 5 h [13].

Synthesize of β -Wollastonite (β -CaSiO₃): β -wollastonite was synthesized by mixing of CaO and SiO₂ with 1:1 w/w ratio [14]. Distilled water was added to the mixtures under vigorous mixing at 500 rpm and temperature of 70 °C for 4 h. The resulting solution was kept at room temperature for 24 h and then decanted to obtain a precipitate. The precipitate was dried in an oven for 20 h at a temperature of 100 °C and then calcined in an electric furnace at a temperature of 900 °C for 4 h [15]. The prepared materials are kept in an inert atmosphere for subsequent characterization and manufacturing of the ceramic tile.

Manufacturing of Ceramic Tiles: Clay was separated manually from its impurities and soaked in water for three days and washed to remove unwanted matter. Then, it was dried for overnight in an oven at 105 °C and then introduced into disk mill followed by Ultra centrifugal mill. The powdered clay was then passed through a sieve with a nominal aperture of 75 μm whereas the β -wollastonite was sieved with the nominal aperture of 63, 75 and 125 μm . β -wollastonite was blended with clay at three different proportions (weight percentage) (5%, 15% and 25%). Then, water was poured into the mixture under vigorous mixing until the mixtures were easy to work by hand and allowed to stand for 16 h. The mixtures were cast into rectangular (120 \times 65 \times 8 mm³) formwork (mold) and compacted by applied uniform force. The green tiles formed were then covered and kept in the cupboard for two days in an open air to slowly loss its moisture content. After this, the tiles were opened and then dried at 105 °C in an oven for 24 h. The dried tiles were loaded into the furnace and heated at 5 °C/min until 250 °C and hold at this temperature for 30 min. Then, the temperature was gradually increased to 950, 1000 and 1050 °C at a heating rate of 10 °C/min and allowed for 1 h to ensure complete firing. The tiles were then allowed to cool inside the furnace to room temperature and kept carefully for final characterization and testing.

2.3 Characterization and Material Testing

Fourier Transforms Infrared Spectroscopy (FTIR): FTIR spectroscopic tool is employed to identify the key functional groups of the extracted and synthesized products. Structural changes within the samples. A sample of 1 mg ($<63 \mu\text{m}$) was mixed with 100 mg of KBr and then pressed to prepare the pellets. The FTIR spectrum was recorded over a wavenumber range of $4000\text{--}400 \text{ cm}^{-1}$ with a 4 cm^{-1} resolution and ordinate unit of transmittance (%).

Powder X-ray Diffraction (XRD): The crystalline structure of the synthesized material was characterized via XRD. The X-ray patterns were taken from radiation source $\text{Cu-K}\alpha 1$ ($\lambda = 1.540593 \text{ \AA}$) by supplying 40 kV to X-ray generator. Spectra were observed from 0 to 60° at a step size of 0.02° .

Linear Shrinkage (LS) Test: The linear shrinkage test was determined for fired ceramic tile samples. The tiles length of the green body and the fired body was measured and determined using ASTM C356-03 method [16].

Water Absorption (WA) Test: The fired ceramic tiles were weighed, immersed in water and boiled for 2 h. Then, it was cooled to room temperature and stand for 12 h. The tiles then removed and the surface water wiped off and weighed. The absorption was determined using ASTM C373-88 method [17].

Acid Resistance Test (ART): To analyze the ceramic specimen's acid resistance test, the specimens were crushed and sieved in 2 mm sieve. Then, weigh a 10 g of crushed tile samples and immersed into 25 ml of acidic solution ($0.5 \text{ M H}_2\text{SO}_4$) at 80°C for 48 h. After this treatment, the specimens were successively washed with distilled water, dried at 80°C for 24 h and weighed [18];

$$\text{Weight Loss (\%)} = \frac{\text{Initial weight} - \text{Final weight}}{\text{Initial weight}} \times 100 \quad (3)$$

Compressive Strength (CS) Test: The compressive strength tests of the ceramic tiles were carried out using the compressive testing machine (Model: BN62223/2000). The compressive strength of the ceramic tiles determined using Eq. 4 [19];

$$\text{Compressive strength (CS)} = \frac{\text{Crushig load}}{\text{Effective surface area of tile}} \quad (4)$$

3 Results and Discussions

3.1 Characterization of the Precursor Materials and β -Wollastonite

FTIR Spectra Analysis: The major functional groups present in silica powder were identified by the FTIR spectra as shown in Fig. 1(a). The broadband at 3440 cm^{-1} is due to silanol hydroxyl groups (responsible for the surface OH groups of $-\text{Si}-\text{OH}$). The absorption peak at 1638 cm^{-1} is attributed to the adsorbed water (HOH) bending

vibration mode. The water has no substantial effect on the structure of the silica powder. The peak at 1103 and 620 cm^{-1} are associated with Si–O–Si asymmetrical and symmetrical stretch vibration mode, respectively. The peak at 486 cm^{-1} is attributed to the asymmetric bending vibration mode of a Si–O–Si bond [20, 21].

Figure 1(b) shows the FTIR spectra of lime. The broadband at 1426 cm^{-1} shown the vibrational stretching of Ca–O. The sharp peak at 874 cm^{-1} was assigned to the characteristic vibration bending of the Ca–O groups. [22]. The β -Wollastonite (Fig. 1(c)) exhibited characteristic absorption bands for the vibrational bending mode of Si–O–Si and O–Si–O at 567 cm^{-1} , the vibrational stretching mode of O–Si–O at 825 cm^{-1} , vibrational mode of Si–O–Ca appeared at 1026 cm^{-1} and the vibrational stretching modes of Si–O–Si at 1115 cm^{-1} . The peak at around 1456 cm^{-1} is due to the existence of Ca–O in the structure. The broadband at about 3440 cm^{-1} in the product can be assigned to stretching vibration of Si–OH group [23].

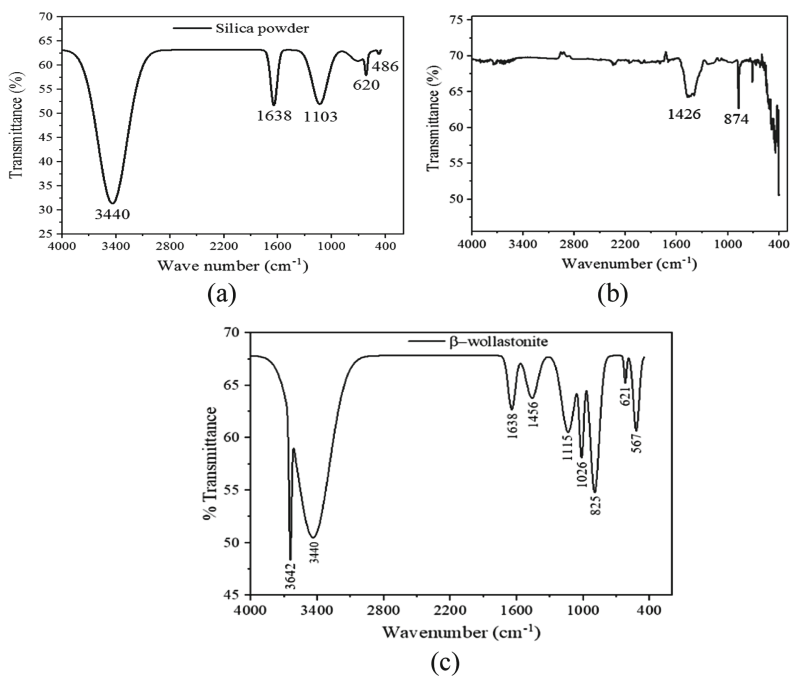


Fig. 1. FTIR spectra of (a) silica, (b) lime and (c) β -wollastonite

Powder X-ray Diffraction (XRD): The silica powder contained both the crystals (quartz) and an amorphous phase as shown in Fig. 2a. The sharper strong broad peaks were observed at $2\theta = 19.68^\circ, 20.18^\circ, 20.92^\circ, 21.4^\circ, 27.7^\circ, 29.38^\circ, 31.34^\circ, 33.1^\circ, 33.98^\circ, 36.68^\circ, 37.78^\circ$ and 40.86° . The major peaks of crystalline quartz occur at 2θ angles of 21.40° ($d = 4.15\text{ \AA}$) which corresponds to a crystalline structure [24]. Figure 2b shows the powder X-Ray Diffraction pattern of lime. The lime was in the crystalline phase with one strong sharp peak and many low-intensity peaks. As can be seen in the figure,

the peaks are observed at 2θ of 23.30° , 28.32° , 31.76° , 34.66° , 39.36° , 41.28° , 44.68° , 48.46° , 52.72° , 53.76° and 56.08° . The major peak was observed at 2θ equal to 34.66° ($d = 2.59 \text{ \AA}$).

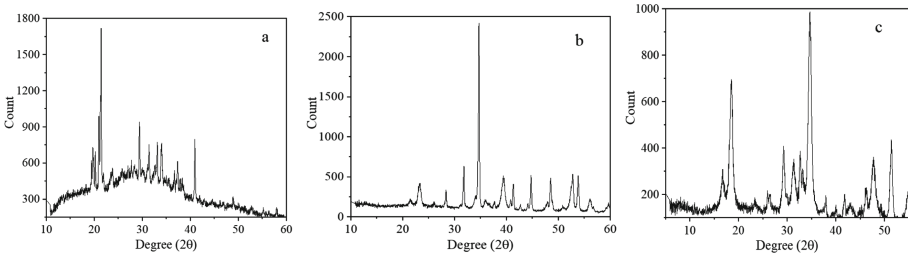


Fig. 2. X-Ray Diffraction of silica (a), lime (b) and β -wollastonite (c)

The phase formation behavior of β -wollastonite during calcination process was investigated using XRD as shown in Fig. 2c. It seems that almost all peaks were related to triclinic β -wollastonite of maximum relative intensity (98.8%) at a diffraction angle of 2θ equal to 34.5° ($d = 2.6 \text{ \AA}$), with the small amount of amorphous phase. The peaks obtained for β -wollastonite from XRD results at 2θ are 16.56° , 18.3° , 29.1° , 31.2° , 32.51° , 33.01° , 34.5° , 41.62° , 45.93° , 47.63° and 51.22° .

3.2 Effect of Operating Conditions on Ceramic Tile Properties

Effect of Operating Conditions on Linear Shrinkage

As it can be seen in Fig. 3a, the linear shrinkage of ceramic tile is increased with the firing temperature. The average values are 3.47%, 4.54% and 6.06% for firing temperature of 950°C , 1000°C and 1050°C , respectively. A similar result have been reported elsewhere [25, 26] that the linear shrinkage of ceramic tiles is increased with the firing temperature. In contrast, linear shrinkage is decreased as the particle size increased (Fig. 3a) because coarse particle requires more energy and time to complete densification. Besides, a coarse particle has a small specific surface area which limit the densification process [27]. The average values are 5.32%, 4.77% and 3.98% for the particle size of 63, 75 and $125 \mu\text{m}$, respectively.

The average linear shrinkage values are 6.53%, 4.68% and 2.87% for 5%, 15% and 25% of β -Wollastonite concentration, respectively (Fig. 3b). It seems that the ceramic tiles with high β -wollastonite concentration exhibited low linear shrinkage because of the low shrinkable tendency of β -wollastonite mineral [28, 29]. The linear shrinkage is decreased when the ratio of β -wollastonite to clay increased even at high firing temperature (1050°C). Since, the formation of calcium aluminosilicates seems to involve a smaller amount of liquid phase during sintering, thereby resulting in a smaller firing shrinkage [30]. One of the methods for controlling firing shrinkage is the use of various calcium-containing materials [31].

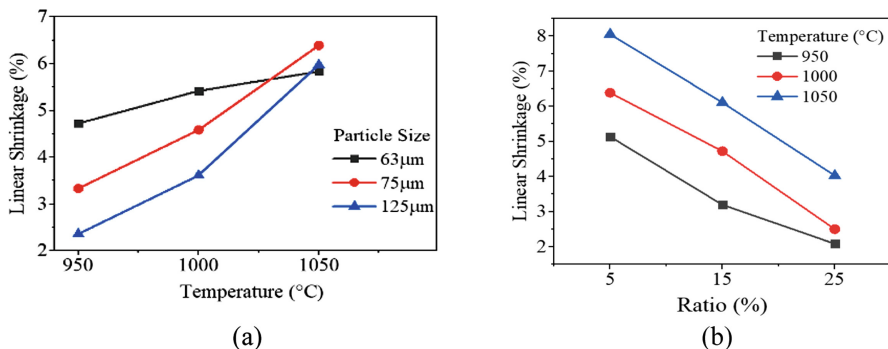


Fig. 3. Effect of firing temperature and particle sizes (a) and ratio of β -Wollastonite and firing temperature (b) on the linear shrinkage of ceramic tiles for different

Effect of Operating Conditions on Water Absorption

The result of water absorption of ceramic tiles is shown in Fig. 4(a) and (b). As it can be seen in Fig. 4(a), the water absorption of ceramic tiles decreased from 23.57% (15.47% to 11.82%) to 64.15% (11.82% to 4.24%), when the temperature increases from 950 °C to 1050 °C. The pore present in ceramic bodies during ceramic processing is filled due to the grain starts growing in the hole part of the ceramic body. The lower temperature used was insufficient to promote densification and consequently, promote substantial closing the porosity.

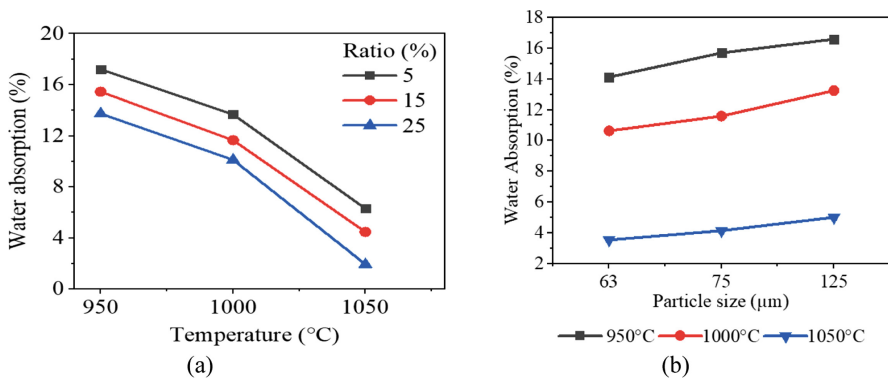


Fig. 4. Effect of firing temperature and ratio of β -Wollastonite (a) and particle size of β -wollastonite and firing temperature (b) on the water absorption of ceramic tiles

The water absorption of ceramic tiles is directly related to porosity and decreased when the firing temperature is increased [32]. Similarly, the water absorption is reduced by 30.6% (12.4, 10.53 and 8.6%) when the ratio of β -wollastonite increased from 5 to 25% (Fig. 4(a)). The presence of β -wollastonite in a high concentration increases the green body density during pressing and reduces the formation of pinholes in the firing stage, as a result, water absorption is decreased [33].

The average water absorption of ceramic tiles is 9.43%, 10.48% and 11.62% for particle size of 63, 75 and 125 μm , respectively (Fig. 4(b)). The water absorption increased with the particle size because of the coarse particle are less compacted and encourage the formation of voids in casting and pressing stages, as a result, it is easy to create pinholes at firing stage. Vieira and Monteiro were found that the water absorption of ceramic tiles is increased with the particle size of starting materials [34]. When the firing temperature raised from 950 to 1050 $^{\circ}\text{C}$ the water absorption of ceramic tiles is decreased from 14.12% to 3.55%, 15.69% to 4.15% and 16.59% to 5.02 for particle size 63 μm , 75 μm and 125 μm , respectively. During firing stage, fine particle accelerates the densification process, decreasing the open porosity as compared to ceramic tiles contained coarse particles of β -wollastonite.

Effect of Operating Conditions on Acid Resistance

Figure 5a shows the weight losses of ceramic tile samples are increased with firing temperature. The average weight losses of ceramic samples are 0.031%, 0.043% and 0.063% for firing temperature of 950 $^{\circ}\text{C}$, 1000 $^{\circ}\text{C}$ and 1050 $^{\circ}\text{C}$, respectively. The firing temperature raised from 950 to 1050 $^{\circ}\text{C}$ the internal structure of ceramic tiles was started deformation and phase change. As a result, the amorphous phase easily attacked by acid solution than the crystalline phase. The acid resistance of ceramic tiles is decreased when the firing temperature increased. This is due to the phase of the ceramic starting materials have a tendency to form the amorphous phase [18].

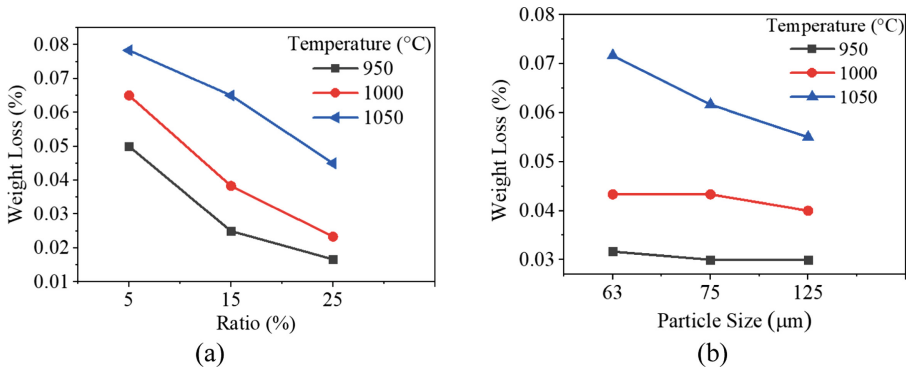


Fig. 5. Effect of firing temperature and ratio of β -wollastonite (a) and particle size of β -wollastonite and firing temperature (b) on the acid resistance of ceramic tiles

During acid etching, the alkaline metal (Ca^{2+}) ion replaced by H^{+} ion and more silica-rich layer formation on the ceramic specimens. However, the concentration of β -wollastonite increased directly implies the Ca^{2+} ion concentration in the ceramic tile fabrication gives protection from the acidic condition. Because, if there is an excess alkaline metal ion present in the samples the H^{+} ions are saturated and no more reaction takes place. The average weight losses of ceramic tile samples are 0.064%, 0.043% and 0.029% for 5, 15 and 25% concentration of β -wollastonite, respectively. The amount of β -wollastonite in the ceramic tile's compositions played a great role in both acid resistance and cleanability by alkaline detergent solutions [35].

Figure 5b shows the variation of the weight loss within the particle size of β -wollastonite. This test was conducted with the same particle size of ceramic tile samples (2 mm). However, the starting materials of ceramic tiles were in three different particle size of β -wollastonite (63, 75 and 125 μm). Therefore, this small variation in the acid resistance test result is due to the variation of the particle size of starting materials. The fine particles are easy to attack by acid solution compared to coarse particle since fine particle has a large specific surface area [36].

Effect of Operating Conditions on Compressive Strength

The average values are 17.21, 20.86 and 26.54 MPa for the firing temperature of 950, 1000 and 1050 $^{\circ}\text{C}$, respectively (Fig. 6a). When the firing temperature increased the porosity of the specimens decreased for inorganic reinforcement fillers. The previous study confirms that the ceramic tiles which contain inorganic reinforcement filler, the compressive strength increased with firing temperature due to better densification [31].

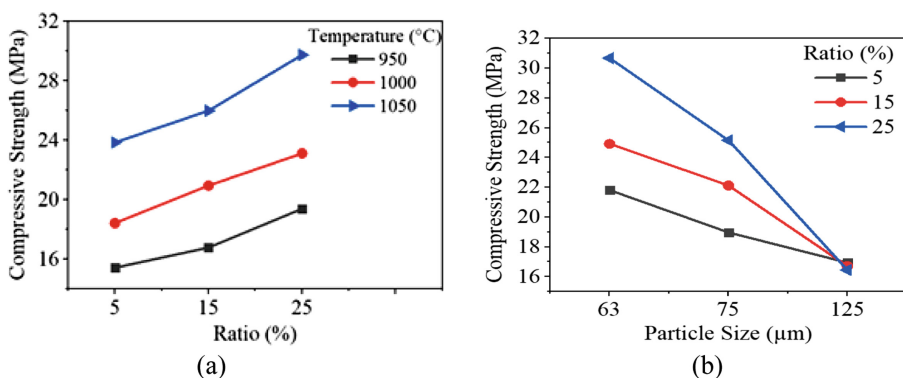


Fig. 6. Effect of firing temperature and ratio of β -Wollastonite (a) and particle size of β -Wollastonite and firing temperature (a) on the compressive strength of ceramic tiles

Moreover, there is no thermal transformation of clay to mullite below 1050 $^{\circ}\text{C}$, mechanical strength decreases as a result of the presence of mullite [37]. On the other hand, anorthite forms from β -wollastonite and alumina at a temperature of 1025 $^{\circ}\text{C}$. Anorthite ($\text{CaAl}_2\text{Si}_2\text{O}_8$) is considered the most effective mineral in increasing the mechanical strength of ceramic materials [38]. Consequently, the formation of anorthite is responsible for increasing the strength after adding 25% of β -Wollastonite. The average values of compressive strength for addition of 5, 15 and 25% ratio of β -Wollastonite is 19.24, 21.28 and 24.09 MPa, respectively (Fig. 6a). This implies that the compressive strength of ceramic tile is increased with the ratio of β -Wollastonite which densifies the microstructure of the ceramic tile matrix [39].

The compressive strength of ceramic tiles is decreased when the particle size of β -Wollastonite increased from 63 to 125 μm (Fig. 5b). The average values are 25.8, 22.08 and 16.73 MPa for 63, 75 and 125 μm particle size of β -Wollastonite, respectively. Many researchers agreed that the particle size and particle-size distribution directly influence the porosity which influences the compressive strength [40]. The similar finding also

reported as the possibility of increasing the compressive strength (or decreasing porosity) by using a fine particle size or an optimized combination of different particle sizes is well known from other technical fields [41].

The fine particles under the influence of high temperature bonded by the particle-dissolving action and the grain grow between the particles and ultimately bond the particles together. As the boundaries between grains grow, porosity progressively decreases and pores close off.

4 Conclusion

In this study β -wollastonite was synthesized from lime and silica obtained from rice husk was tested as filler for ceramic tile production. It was found that silica as a precursor material for β -wollastonite was successfully extracted from rice husk by using alkaline extraction followed by acid precipitation with a yield of 91.34%. The synthesized β -wollastonite material with different proportion of clay was used to fabricate the ceramic tiles. Besides, the effect of particle size and firing temperature on the quality of final product was investigated. It was observed that percentage of β -wollastonite, firing temperature and particle size have an important effect on the quality of the fabricated ceramic tile. It was found that the fabricated ceramic tiles reinforced with β -wollastonite have an acceptable material property for the intended application.

References

1. Wattanasiriwech, D., Saiton, A., Wattanasiriwech, S.: Paving blocks from ceramic tile production waste. *J. Clean. Prod.* **17**, 1663–1668 (2009)
2. Saleiro, G., Holanda, J.: Processing of red ceramic using a fast-firing cycle. *Cerâmica* **58**(347), 393–399 (2012)
3. El Ouahabi, M., et al.: Potentiality of clay raw materials from northern Morocco in ceramic industry: Tetouan and Meknes areas. *J. Miner. Mater. Charact. Eng.* **2**, 145–159 (2014)
4. Glymond, D., et al.: Production of ceramics from coal furnace bottom ash. *Ceram. Int.* **44**, 3009–3014 (2016)
5. Darsana, P., et al.: Development of coir-fibre cement composite roofing tiles. *Procedia Technol.* **24**, 169–178 (2016)
6. Lawrence, J., Li, L., Spencer, J.: A two-stage ceramic tile grout sealing process using a high power diode laser—II. Mechanical, chemical and physical properties. *Opt. Laser Technol.* **30**(3–4), 215–223 (1998)
7. Gennaro, R., et al.: Influence of zeolites on sintering and technological properties of porcelain stoneware tiles. *J. Eur. Ceram. Soc.* **23**(13), 2237–2245 (2003)
8. Podporska, J., et al.: A novel ceramic material with medical application. *Process. Appl. Ceram.* **2**(1), 19–22 (2008)
9. Kamath, S.R., Proctor, A.: Silica gel from rice hull ash: preparation and characterization. *Cereal Chem.* **75**(75), 484–487 (1998)
10. Jembere, A.L., Fanta, S.W.: Studies on the synthesis of silica powder from rice husk ash as reinforcement filler in rubber tire tread part: replacement of commercial precipitated silica. *Int. J. Mater. Sci. Appl.* **6**(1), 37–44 (2017). <https://doi.org/10.11648/j.ijmsa.20170601.16>
11. Della, V.P., Kühn, I., Hotza, D.: Rice husk ash as an alternate source for active silica production. *Mater. Lett.* **57**(4), 818–821 (2002)

12. Todkar, B., Deorukhar, O., Deshmukh, S.: Extraction of silica from rice husk. *Int. J. Eng. Res. Dev.* **12**, 69–74 (2016)
13. Obeid, M.M.: Crystallization of synthetic wollastonite prepared from local raw materials. *Int. J. Mater. Chem.* **4**(4), 79–87 (2014)
14. Obradović, N., et al.: Influence of different pore-forming agents on wollastonite microstructures and adsorption capacities. *Ceram. Int.* **43**(10), 7461–7468 (2017)
15. Noor, A.H.M., et al.: Synthesis and characterization of wollastonite glass-ceramics from eggshell and waste glass. *J. Solid St. Sci. Technol. Lett.* **16**, 1–5 (2015)
16. ASTM C356-03: Standard Test Method for Linear Shrinkage of Preformed High-Temperature Thermal Insulation Subjected to Soaking Heat. *Annual Book of ASTM Standards*, **04**(06), ASTM, West Conshohocken, PA (2000)
17. ASTM C373-88: Standard Test Method for Water Absorption, Bulk Density, Apparent Porosity, and Apparent Specific Gravity of Fired Whiteware Products. *Annual Book of ASTM Standards*, **15**(02). ASTM, West Conshohocken, PA (2005)
18. Kim, B.-H., et al.: Chemical durability of β -wollastonite-reinforced glass-ceramics prepared from waste fluorescent glass and calcium carbonate. *Mater. Sci. Pol.* **22**(2), 83–91 (2004)
19. Odeyemi, S.O., et al.: compressive strength of manual and machine compacted sandcrete hollow blocks produced from brands of Nigerian cement. *Am. J. Civ. Eng.* **3**, 6–9 (2015)
20. Nariyal, R.K., Kothari, P., Bisht, B.: FTIR measurements of SiO₂ glass prepared by sol-gel technique. *Chem. Sci. Trans.* **3**(3), 1064–1066 (2014)
21. Anjaneyulu, U., Sasikumar, S.: Bioactive nanocrystalline wollastonite synthesized by sol-gel combustion method by using eggshell waste as calcium source. *Bull. Mater. Sci.* **37**, 207–212 (2014)
22. Puntharod, R., et al.: Synthesis and characterization of wollastonite from egg shell and diatomite by the hydrothermal method. *J. Ceram. Process. Res.* **14**(2), 198–201 (2013)
23. Morsy, R., Abuelkhair, R., Elnimr, T.: Synthesis of microcrystalline wollastonite bioceramics and evolution of bioactivity. *Silicon* **9**, 489–493 (2017)
24. Liou, T.-H.: Preparation and characterization of nano-structured silica from rice husk. *Mater. Sci. Eng. A* **364**(1–2), 313–323 (2004)
25. Karaman, S., Ersahin, S., Gunal, H.: Firing temperature and firing time influence on mechanical and physical properties of clay bricks. *J. Sci. Ind. Res.* **65**, 153–159 (2006)
26. Klaytae, T., et al.: The effects of sintering temperature on the physical and electrical properties of SrTiO₃ ceramics prepared via sol-gel combustion method. *Ferroelectrics* **491**(1), 79–86 (2016)
27. Bin, Z., et al.: The effect of particle size on the properties of alumina-based ceramic core. In: Zhouzhou, Y., Luo, Q. (eds.) *Applied Mechanics and Materials*. Trans Tech Publications, Zürich (2011)
28. Demidenko, N.I., et al.: Wollastonite as a new kind of natural material (a review). *Sci. Ceram. Prod.* **58**(9), 308–311 (2001)
29. Turkmen, O., Kucuk, A., Akpinar, S.: Effect of wollastonite addition on sintering of hard porcelain. *Ceram. Int.* **41**(4), 5505–5512 (2015)
30. Lira, C., et al.: Effect of carbonates on firing shrinkage and on moisture expansion of porous ceramic tiles. In: *V World Congress on Ceramic Tile Quality-Qualicer* (1998)
31. Das, S.K., et al.: Shrinkage and strength behaviour of quartzitic and kaolinitic clays in wall tile compositions. *Appl. Clay Sci.* **29**(2), 137–143 (2005)
32. Lin, K.-L., Lee, T.-C., Hwang, C.-L.: Effects of sintering temperature on the characteristics of solar panel waste glass in the production of ceramic tiles. *J. Mater. Cycles Waste Manage.* **17**(1), 194–200 (2015)
33. Tiggemann, H.M., et al.: Use of wollastonite in a thermoplastic elastomer composition. *Polym. Test.* **32**(8), 1373–1378 (2013)

34. Vieira, C.M.F., Monteiro, S.N.: Effect of the particle size of the grog on the properties and microstructure of bricks. In: Salgado, L., Filho, F.A. (eds.) *Materials Science Forum*. Trans Tech Publications, Zürich (2006)
35. Hupa, L., et al.: Chemical resistance and cleanability of glazed surfaces. *Surf. Sci.* **584**(1), 113–118 (2005)
36. Meddah, M.S., Zitouni, S., Belâabes, S.: Effect of content and particle size distribution of coarse aggregate on the compressive strength of concrete. *Constr. Build. Mater.* **24**(4), 505–512 (2010)
37. Junior, A.D.N., et al.: Influence of composition on mechanical behaviour of porcelain tile. Part II: mechanical properties and microscopic residual stress. *Mater. Sci. Eng. A* **527**(7–8), 1736–1743 (2010)
38. Kurama, S., Ozel, E.: The influence of different CaO source in the production of anorthite ceramics. *Ceram. Int.* **35**(2), 827–830 (2009)
39. Wahab, M.A., et al.: The use of Wollastonite to enhance the mechanical properties of mortar mixes. *Constr. Build. Mater.* **152**, 304–309 (2017)
40. Isabella, C., et al.: The effect of aggregate particle size on formation of geopolymeric gel (2003)
41. Spath, S., Drescher, P., Seitz, H.: Impact of particle size of ceramic granule blends on mechanical strength and porosity of 3D printed scaffolds. *Materials* **8**, 4720–4732 (2015)